Available online at www.sciencedirect.com

ScienceDirect

Geochimica et Cosmochimica Acta 125 (2014) 539–550

Geochimica et Cosmochimica Acta

www.elsevier.com/locate/gca

# Both soluble and colloidal iron phases control dissolved iron variability in the tropical North Atlantic Ocean

Jessica N. Fitzsimmons [a,b,*], Edward A. Boyle [b]

[a] MIT/WHOI Joint Program in Chemical Oceanography, MIT E25-615, 45 Carleton St, Cambridge, MA 02142, USA
[b] Massachusetts Institute of Technology, MIT E25, 45 Carleton St, Cambridge, MA 02142, USA

Received 25 June 2013; accepted in revised form 19 October 2013; Available online 30 October 2013

**Abstract**

The size partitioning of dissolved iron (dFe, <0.4 μm) into soluble (sFe, <0.02 μm) and colloidal (0.02 μm < cFe < 0.4 μm) phases was investigated at seven stations in the tropical North Atlantic Ocean, and the results are compared to the dFe size fractionation study of Bergquist et al. (2007) in the same region. Downwind of the North African dust plumes, cFe comprised 80 ± 7% of the surface dFe pool at six stations, supporting the hypothesis that atmospherically-derived Fe is maintained in the colloidal size fraction. At the deep chlorophyll maximum, colloidal Fe had minimum concentrations or was completely absent, suggesting that cFe was either preferentially taken up by microbes and/or scavenged/aggregated at these depths. At remineralization depths, sFe was the dominant fraction both in the subtropical gyre-like stations (76% sFe; [sFe] = 0.42 ± 0.03 nmol/kg) and in the oxygen minimum zone (56% sFe; [sFe] = 0.65 ± 0.03 nmol/kg). Only at remineralization depths of stations with intermediate oxygen concentrations (100–110 μmol/kg) did colloidal Fe dominate (contributing 58% of dFe) , indicating that cFe may be serving as a conduit of dFe loss during mixing of high-Fe OMZ and low-Fe gyre waters. North Atlantic Deep Water (NADW) had a typical sFe concentration of 0.34 ± 0.05 nmol/kg. In the deepest samples composed of a NADW/Antarctic Bottom Water mixture where the bottom water may have attained a ~0.1 nmol/kg hydrothermal Fe input during transit past the Mid-Atlantic Ridge, sFe did not increase coincidentally with dFe, indicating that any potential hydrothermal Fe contribution was colloidal. In general, the results of this study counter the previous hypothesis of Bergquist et al. (2007) that the colloidal Fe fraction predominately controls dFe variability, instead suggesting that both soluble and colloidal Fe are variable, and both contribute to the observed dFe variability throughout the North Atlantic. The nearly 50–50% dFe partitioning into soluble and colloidal phases below the DCM suggest one of two partitioning mechanisms persists: (1) soluble and colloidal Fe exchange rates reach a "steady state," over which regional, uniquely-partitioned Fe sources can be overlain, or (2) the partitioning of Fe-binding ligands between the two size fractions is variable in the open ocean and directly controls dFe partitioning.


## 1. INTRODUCTION

For decades an understanding of the limitation of marine primary productivity by the micronutrient iron (Fe; Martin and Fitzwater, 1988; Morel et al., 2003) has been hampered by the scant knowledge of its global distribution. With the advent of the international GEOTRACES program, however, global transects of dissolved Fe (dFe) are being measured, and the new data will generate a much improved understanding of the sources and sinks of this important micronutrient. These developments will allow a shift in the objectives of trace metal research from establishing the distribution of trace metals to determining the processes that control those distributions. One such process, the transfer of metals from the dissolved pool into the

* Corresponding author at: MIT E25-615, 45 Carleton St, Cambridge, MA 02142, USA. Tel.: +1 617 324 0283; fax: +1 617 2538630.
*E-mail address:* jessfitzsimmons@gmail.com (J.N. Fitzsimmons).

0016-7037/$ - see front matter © 2013 Elsevier Ltd. All rights reserved.
http://dx.doi.org/10.1016/j.gca.2013.10.032

sinking particulate pool ("scavenging"), is in particular need of illumination. Several metal loss mechanisms are encompassed by the term "scavenging," including adsorption/surface complexation, precipitation, and aggregation into successively larger particles, as well as microbiological uptake.

Colloids, the focus of this study, are an understudied physico-chemical group of compounds defined as particles so small that they are operationally included in the dissolved size fraction, but they retain their status as particles because they are physically distinct from the fluid via a surface boundary. Because of their diminutive size, colloids remain suspended until they aggregate to a size experiencing significant gravitational settling. Colloids thus serve the important role of transporting material between the dissolved and sinking particulate phases, thereby coupling two of the aforementioned "scavenging" processes: a rapid initial adsorption of dissolved metal onto colloidal/particulate material in solution, followed by a slow aggregation of the colloids into particulate material of filterable size (the Brownian-pumping model, Honeyman and Santschi, 1989). Additionally, while suspended, colloidal material can mediate chemical processes that further alter the bulk seawater solution including sorption of solutes, ligand exchange, surface redox reactions, and photochemical reactions.

For Fe, a hybrid-type element demonstrating both nutrient-type profile shapes as well as scavenged-type surface maxima and concentration loss along global thermohaline circulation (Bruland and Lohan, 2003), scavenging plays an important role in its marine biogeochemical cycle. Under oxic conditions, Fe(III) has a very low inorganic solubility in seawater (Millero, 1998). Instead, marine dissolved Fe is complexed by natural organic ligands that elevate dFe concentrations above the <0.1 nM solubility observed in UV-irradiated seawater (Kuma et al., 1996; Liu and Millero, 2002)., while excess Fe above these ligand concentrations is rapidly precipitated. Of this marine dFe, a large fraction, often 30–70% and as high as 90%, of the dissolved Fe in the ocean exists in the colloidal size fraction (Wu et al., 2001), which is operationally defined in this study as the dFe between 0.02 μm and 0.4 μm (cFe, "colloidal Fe", and "Fe colloids" will be used interchangeably in this paper; soluble Fe, sFe, is the Fe passing through a 0.02 μm filter; sFe + cFe = dFe). Thus, although dissolved Fe is classically envisioned as bound to soluble, siderophore-like organic ligands in seawater, a large portion of marine dFe is actually composed of tiny particles (colloids) that may have a different chemical composition and behavior than truly dissolved (soluble) Fe.

Using transmission electron microscopy imaging and energy dispersive spectroscopy composition analyses, it was concluded that colloidal Fe is organically bound in the open ocean (Wells and Goldberg, 1991, 1992). This is consistent with electrochemical measurements of Fe ligand concentration and binding strength that indicate that >99% of marine dFe, which contains the colloidal fraction, is bound by organic Fe-binding ligands (Rue and Bruland, 1995; Gledhill and Buck, 2012). However, due to their differences in size and chemical composition, soluble and colloidal Fe have unique behaviors that affect the Fe biogeochemical cycle in two ways. First, because soluble and colloidal Fe undergo different chemical transformations (sFe experiencing sorption and cFe experiencing aggregation), the two phases may have inherently different residence times. Thus, the measured size partitioning at any site could influence, for instance, whether new dFe sources escape abiotic scavenging long enough to be taken up by microbes, and consequently modelers must understand the size distribution of dFe in order to best predict dFe concentrations down current.

Second, and even more important to studies of micronutrient limitation, soluble and colloidal Fe may not be equally bioavailable. Laboratory experiments have conclusively shown that inorganic Fe colloids (here called nanoparticles) as small as 6–50 Fe atoms per colloid are not directly bioavailable to diatoms (Rich and Morel, 1990). However, since most marine colloidal Fe is thought to be organically bound, incubations using natural, organic-dominated colloidal Fe assemblages were also executed to reflect more realistic marine compounds, and the results indicated that natural colloidal Fe is only indirectly bioavailable, requiring first a dissociation from the colloid into the soluble phase before being taken into the cell. The smaller soluble Fe fraction, in contrast, was always taken up faster and is thus thought to be preferred (Chen and Wang, 2001). An assessment of the bioavailability of natural colloidal Fe is essential in order to ensure that nutrient limitation models do not underestimate the geographic extent of Fe limitation simply because they parameterize the bioavailable Fe pool as dFe instead of sFe.

In their Atlantic Ocean size partitioning study of dFe, Bergquist et al. (2007) concluded that much of the dFe variability in the tropical and subtropical Atlantic Ocean was due to a dynamic colloidal fraction, while the soluble Fe concentration remained relatively constant with depth. This highlighted the importance of studying dFe size partitioning, as it suggested that the cycling of the two size fractions is distinct. In this study, we have measured dFe size partitioning at several more stations across the tropical North Atlantic, reaching further along the southwestern boundary of the subtropical gyre and east into the heart of the oxygen minimum zone (OMZ). We find that both soluble and colloidal fractions determine the dissolved Fe variability in this broader region, instead of just the colloidal fraction as in Bergquist et al.'s study. In this paper we will establish the similarities and differences between the Bergquist et al. study and the new data presented here, and we will attempt to illuminate the major facets of dFe size partitioning and its contribution to Fe biogeochemistry in the tropical North Atlantic.

## 2. SAMPLING & ANALYSIS METHODOLOGY

In August 2008, trace metal clean seawater samples were collected aboard the *R/V Oceanus* (cruise OC449-2 sailing from Bridgetown, Barbados, to Mindelo, Cape Verde Islands) in the tropical North Atlantic (see cruise track in Fig. 1). A review of the sample collection and Fe analysis protocols for this cruise can be found in Fitzsimmons

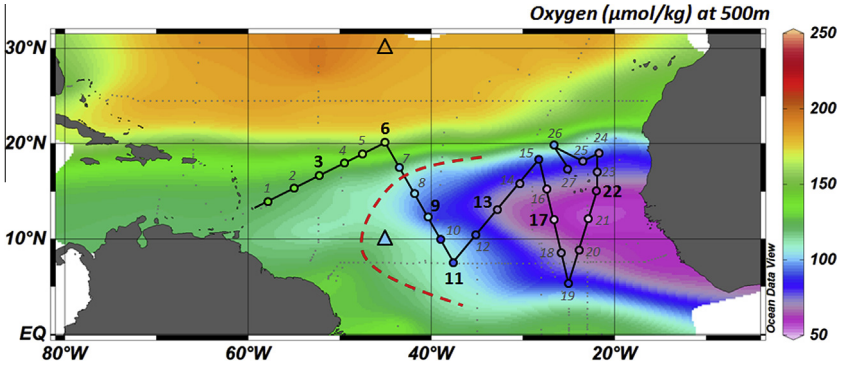


Fig. 1. OC449-2 cruise track with the seven stations sampled for dFe size partitioning indicated in bold. Color contours indicate the distribution of dissolved oxygen at 500 m taken from the eWOCE dataset (small dots). Colors inside the station dots indicate the dissolved oxygen concentrations at 500 m measured on OC449-2. The two triangles designate the subtropical gyre station (30°N, 45°W) and the OMZ station (10°N, 35°W) from Bergquist et al. (2007). The dashed red line designates the cut-off used in this study between the assigned "subtropical gyre stations" (3 & 6) and "OMZ stations" (9, 11, 13, 17, & 22). (For interpretation of the references to color in this figure legend, the reader is referred to the web version of this article.)

et al. (2013), which discusses the major processes controlling the dFe distribution along this transect. Briefly, the Moored *In situ* Trace Element Serial Samplers (MITESS, Bell et al., 2002) were used to collected profile seawater samples in the "Vane" mode using deployment procedures described in Fitzsimmons and Boyle (2012). Near-surface samples (~5 m depth) were collected using the Automated Trace Element ("ATE") sampler, which is a single MITESS unit deployed manually off the side of the ship using a plastic-coated line. Seawater was vacuum-filtered (0.5 atm.) through 0.4 μm Nuclepore™ filters on a Savillex™ fluorocarbon filter rig directly into acid-cleaned 30 mL HDPE sub-sampling bottles after two rinses. MITESS Vane sample collection produced dFe concentrations indistinguishable from those collected by the US GEOTRACES GO-FLO carousel system (Fitzsimmons and Boyle, 2012).

To collect sFe samples, a 0.02 μm Anodisc filter was pre-cleaned on a Teflon filter rig first with >100 mL pH 1.5 HCl (distilled 4× in a Vycor still and tested for trace metal purity), followed by >100 mL trace metal-clean distilled water, and finally ~50 mL unfiltered seawater sample, after which unfiltered seawater was passed through the clean Anodisc filter and collected as sFe into acid-cleaned 30 mL HDPE sub-sampling bottles after one bottle rinse. Samples were acidified at sea to pH 2, and at least six months after acidification they were analyzed in triplicate for their Fe content by isotope dilution inductively-coupled plasma mass spectrometry (ID-ICP-MS) on a hexapole collision cell IsoProbe multiple collector-ICP-MS. The ID-ICP-MS method employs an $^{54}$Fe-spike and batch pre-concentration with nitrilotriacetate resin (Lee et al., 2011). Analyses of SAFe D2 standard for dFe during the period of the OC449-2 seawater analyses averaged $0.95 \pm 0.05$ nmol/kg (Bottle 33, ±1SD, $n = 38$) and $0.90 \pm 0.02$ nmol/kg (Bottle 446, ±1SD, $n = 10$), which agree well with the current consensus value of $0.933 \pm 0.032$ nmol/kg (consensus as of May 2013; www.geotraces.org/science/intercalibration). SAFe S was not analyzed during the period of the OC449-2 analyses but was measured using the same analytical method within 6 months as $0.097 \pm 0.006$ nmol/kg (Bottle 16, ±1SD, $n = 3$), which is identical to the current consensus value of $0.093 \pm 0.008$ nmol/kg.

## 3. RESULTS AND DISCUSSION

### 3.1. Surface distribution

The surface ocean distributions of dFe and sFe as a function of longitude are shown in Fig. 2. As discussed in Fitzsimmons et al. (2013), dFe concentrations in the tropical North Atlantic exhibited maxima at the surface, in accordance with expectations of high aerosol Fe deposition downwind of North Africa along 10–20°N (Mahowald et al., 2005). dFe was highest in the west and lower in the

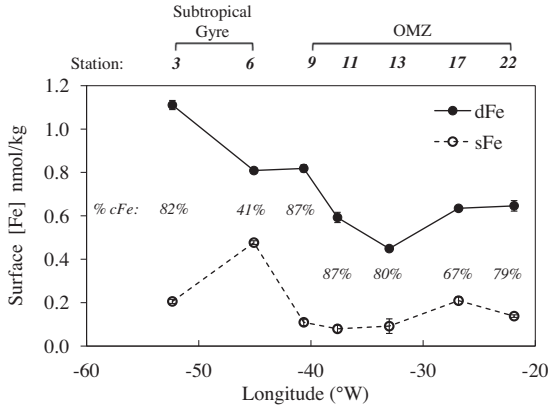


Fig. 2. dFe (solid symbols and lines) and sFe (open symbols, dashed lines) in the surface ocean as a function of longitude, with station numbers and biogeochemical province indicated at the top. Italicized percentages indicate the %cFe contribution to dFe. Error bars are shown for all points and represent ±1σ standard deviation of analytical replicates. Colloidal Fe can be calculated as the difference between dFe and sFe.

east, despite closer proximity to the African dust source; this likely reflects a combination of spatially variable factors including dust source/solubility, dust deposition patterns (seasonal), biological uptake of metals in the surface ocean, and mixed layer depth. NOAA HYSPLIT backward trajectories calculated using the GDAS Meteorological data (shown in the Supplementary material) indicate that the air masses over all of the relevant stations in Fig. 2 originated in NW Africa or Europe, except for Stations 9 & 11 (37–41°W), which had South American sources. It is reasonable to assume that over the 1.5–5 months residence time of dFe in surface waters of the tropical North Atlantic (Bergquist and Boyle, 2006), most of the dFe was derived from North African or European sources.

What is most striking in Fig. 2, however, is that soluble Fe concentrations remained low across the transect (at all but one station) despite a factor-of-two variability in dFe, with sFe $\leqslant$ 0.2 nmol/kg at most stations. Thus, most of the elevated surface dFe was partitioned into the colloidal Fe size fraction (%cFe averaged 80 $\pm$ 7%, with Station 6 removed). This reinforces the hypothesis that atmospherically derived Fe is preferentially maintained in the colloidal pool, which was suggested by Wu et al. (2001) using data near Bermuda and Hawaii and corroborated by Bergquist et al. (2007) in the tropical North Atlantic. It is possible that both soluble and colloidal Fe are released by dust and then sFe is preferentially taken up by microorganisms, resulting in the observed majority of aerosol-derived dFe persisting in the colloidal phase. However, the preferential release of dust-derived Fe into the colloidal size fraction has been shown experimentally via direct leaching of aerosols into filtered seawater containing natural organic Fe-binding ligand assemblages (Aguilar-Islas et al., 2010, although one can be concerned whether excess Fe binding ligands are saturated during these dust leaching experiments, which would generate colloidal Fe oxyhydroxides and bias the resulting size partitioning). Dust-derived Fe colloids could be composed of organically bound Fe-ligand complexes that fall in the colloidal size fraction, colloidal-sized pieces of eroded dust particles, and/or inorganic Fe-colloids formed *in situ* during the dust solubilization process.

In contrast, at the northernmost station of our transect (Station 6: 20°N, 45°W), sFe had a much higher concentration of 0.48 nmol/kg, which exceeded the cFe of 0.33 nmol/kg (59% of the surface dFe was sFe). If dust is assumed to partition into the colloidal fraction, then the decreased cFe contribution at Station 6 could indicate that dust deposition at this northernmost station was reduced. This hypothesis would be supported by a majority partitioning into the soluble phase in the surface ocean of other low-dust regions such as the South Atlantic (Bergquist et al., 2007), subarctic North Pacific (Nishioka et al., 2003), and the Southern Ocean (Boye et al., 2010; Chever et al., 2010). However, the dFe concentration at Station 6 was relatively high (0.8 nmol/kg) and thus requires a recent Fe input. While we cannot exclude that the Station 6 sFe sample might have been contaminated, we also know that dFe is stabilized by organic ligands, and thus the size partitioning of surface Fe-binding ligands at any individual location may be directly controlling the observed partitioning of surface dFe. Only one study has recorded the size partitioning of organic Fe-binding ligands in the tropical North Atlantic (Cullen et al., 2006), with surface water samples taken at one station in the tropical North Atlantic (3.5°N, 44.5°W) and one station in the North Atlantic subtropical gyre (36.1°N, 65°W). At the tropical North Atlantic station, 50–62% of the dissolved ligands fell into the soluble fraction, while at the subtropical gyre station, a higher 72–100% of the dissolved ligands were soluble. Cullen's study demonstrates that ligand partitioning is spatially variable and supports the premise that majority ligand partitioning into the soluble fraction might be predicted in the subtropical gyre, like at our Station 6 which lies closer to the gyre center (with a high surface salinity >37.5 and depressed mixed layer, chlorophyll max, and isopycnals) than any of the other stations sampled on our cruise track. More studies of the size parti-

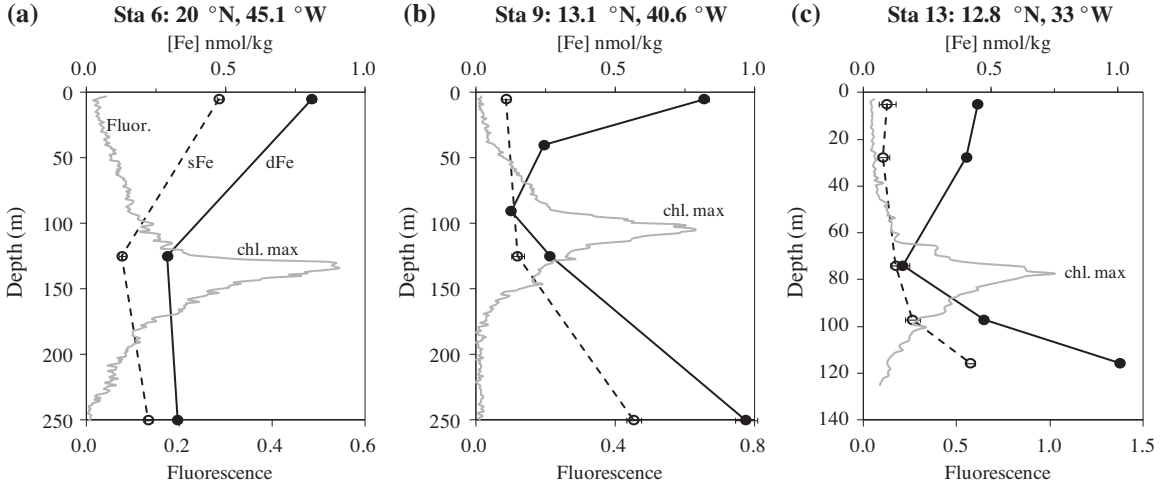


Fig. 3. Euphotic zone dissolved Fe partitioning in the subtropical gyre at Station 6 (a) and in the OMZ at Station 9 (b) and Station 13 (c). dFe is shown in the solid circles (solid line), while sFe is shown in the open circles (dashed line). Error bars are shown for all points and represent $\pm 1\sigma$ standard deviation of analytical replicates. CTD fluorescence (in volts) is shown in gray to indicate the location of the deep chlorophyll maximum. At the OMZ stations, cFe (= dFe–sFe) goes to zero at the chlorophyll maximum.

tioning of Fe-binding ligands across the global ocean would be useful for assessing the impact of the ligand size distribution on the solubility and size partitioning of dFe, especially when comparing high- and low-dust regions. Nevertheless, the predominance of surface colloidal Fe only in regions of significant dust (inorganic Fe) input may also imply that there is a contribution of inorganically bound Fe colloids (nanoparticles) to this dust-derived cFe that is not present in low-dust regions.

### 3.2. Water column profiles

Figs. 3–6 show all of the subsurface dFe and sFe samples collected on OC449-2. Despite the fact that these samples were collected in a relatively narrow 12° latitudinal band, the stations situated farther north and west in the subtropical gyre exhibited very different dFe profiles than those stations farther south and east in the OMZ (Fitzsimmons et al., 2013). Bergquist et al. (2007) made a similar designation of a subtropical gyre (30°N, 45°W) and an OMZ (10°N, 45°W) station (Fig. 1), and the same nomenclature will be applied to the stations in this study's cruise track. Subtropical gyre (3 & 6) and OMZ (9–22) stations were distinguished using salinity profiles (Fig. 4), with subtropical gyre sites having a deeper pycnocline than OMZ stations (Fig. 1). Notably, the stations formed the same groups when sorted by dFe distribution as by pycnocline depth (Fig. 4 a&b), indicating that the biogeochemical signature of each water mass was a determining factor for dFe size partitioning in the tropical North Atlantic.

Dissolved Fe generally displayed a nutrient-type profile with a dust-derived surface maximum, a minimum near the deep chlorophyll maximum (DCM), a maximum in the OMZ, and typical North Atlantic deep water values (Fitzsimmons et al., 2013). The different pools of dFe (cFe and sFe), however, demonstrated unique features with depth. Throughout the open ocean, dFe partitioning can be interpreted as a function of two processes: unique Fe partitioning resulting from individual Fe transformations, inputs, or outputs occurring at the location of interest, and/or a unique Fe ligand partitioning (presumably regulated by microorganisms) that directly regulates the observed dFe partitioning. We will discuss the balance of these two partitioning mechanisms throughout the transect starting in the euphotic zone and extending down to the abyssal ocean.

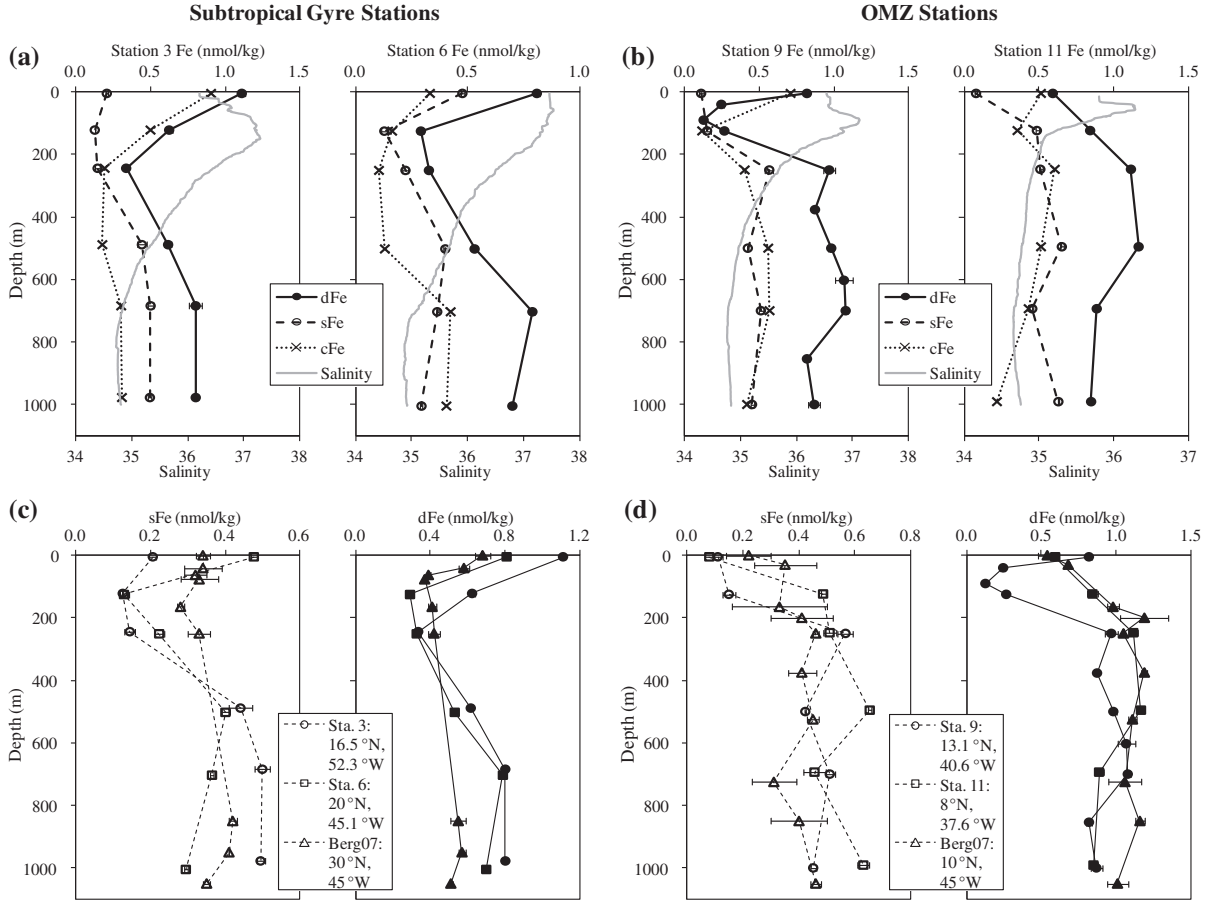


Fig. 4. Dissolved Fe size partitioning to 1000 m in the subtropical gyre (Stations 3 and 6 in a, c) and the OMZ (Stations 9 and 11 in b, d). dFe (filled symbols and solid line), sFe (open symbols, dashed line), and cFe (crossed symbols and dotted line) are shown for individual stations in (a) and (b) with salinity indicated in gray. In (c) and (d), sFe (open symbols, dashed line) and dFe (closed symbols, solid line) profiles from multiple stations are shown together for comparison ("Berg07" data taken from Bergquist et al., 2007). Error bars show ±1σ standard deviations of replicate analyses.

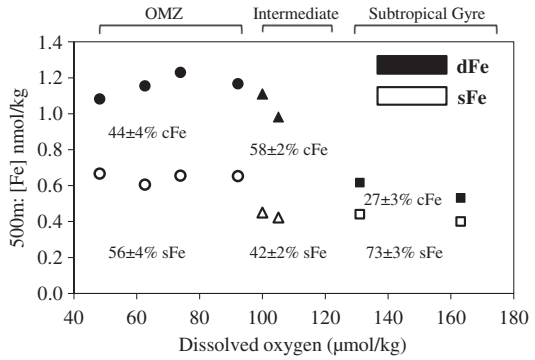


Fig. 5. Dissolved and soluble Fe concentrations at 500 m depth as a function of oxygen concentration. OMZ stations are designated as circles, subtropical gyre stations are designated as squares, and stations with intermediate oxygen concentration are shown as triangles. Note that the data at 100 μmol/kg dissolved oxygen are taken from Bergquist et al. (2007) at 10°N, 45°W. The percentage of dFe composed of soluble or colloidal Fe for each of the three regions is also designated.

### 3.2.1. Euphotic zone

In the euphotic zone, cFe and sFe demonstrated very different profile structures (Fig. 3), suggesting that cFe and sFe behave uniquely in the upper ocean. At all stations, the surface dFe maximum decreased with depth to a minimum near the DCM (Fig. 3). In the subtropical gyre stations, DCM dFe was split between soluble and colloidal fractions (Fig. 3a: Station 6 had 56% cFe), while at the OMZ stations, colloidal Fe disappeared completely in the DCM (Fig. 3b & c). This lack of cFe in the DCM was also observed by Bergquist et al. (2007) at their OMZ station and by Ussher et al. (2010) near the Canary Islands. Chever et al. (2010) also found a cFe minimum in Southern Ocean Antarctic Circumpolar Current (ACC) surface waters that persisted through the upper 100–200 m.

The disappearance of cFe in the DCM could be interpreted as occurring either because of a unique Fe-ligand partitioning in the DCM that is different from that at other depths or as a result of unique Fe transformations occurring in the DCM. If size fractionation of Fe-binding ligands were to explain the observed pattern, the DCM must have had either higher soluble ligand concentrations than colloidal ligands or substantially stronger soluble ligands that outcompeted colloidal ligands for Fe in the DCM. Very few studies have reported the size distribution of Fe-binding ligands at the DCM, but one study in the Southern Ocean ACC found that $92 \pm 3\%$ ($n = 7$) of Fe-binding ligands were soluble in the upper 100 m of water (Boye et al., 2010). This is in contrast to a study near Hawaii that detected almost no soluble ligands in upper 100 m waters (Wu et al., 2001). Regardless, it is generally believed that organic Fe-binding ligands, especially in the upper ocean, are biologically produced (Hunter and Boyd, 2007), and several studies have shown that marine microbes produce "siderophore-like" ligands that would fall into the soluble size fraction (Wilhelm and Trick, 1994; Martinez et al., 2001; Martinez et al., 2003). Thus, it might make sense that strong, "siderophore-like" ligands in the soluble class might be produced at the DCM that outcompete any colloidal ligands present for Fe.

However, without any data defining the Fe-ligand size partitioning in the DCM, an Fe transformation explanation for the observed pattern in Fig. 3 is equally or even more likely. Since the DCM is an upper ocean depth experiencing significant biological activity, it is possible that colloidal Fe is preferentially taken up by microbes, despite observations from incubation studies suggesting that phytoplankton prefer sFe over cFe (Chen and Wang, 2001). Alternatively, protozoan grazer ingestion of cFe could be depressing the cFe concentration at the DCM (Barbeau et al., 1996; Barbeau and Moffett, 2000). Another possible explanation is that because of the particulate maximum in the upper ocean, colloidal Fe may be scavenged onto particles more efficiently at the DCM, or cFe aggregation rates into large particles may be greater at the DCM than at other euphotic zone depths.

It is worth mentioning that at all of the stations where Fe was measured in the DCM, sFe was a measurable 0.10–0.15 nmol/kg. While the tropical North Atlantic is not thought to be Fe-limited, it is not unreasonable to assume that microorganisms would use as much of the sFe as possible, assuming it is more bioavailable. However, we find a persistent $0.13 \pm 0.01$ nmol/kg sFe concentration in the DCM at all stations examined. This pool of sFe may be a relatively refractory Fe pool that is unavailable to marine microorganisms, explaining its persistence. Alternatively, a photochemically-produced Fe(II) pool (Moffett, 2001), either in a pseudo-steady state because of its rapid turnover (high lability) or stabilized by organic ligands (Roy et al., 2008), may also comprise this nearly constant soluble Fe background in the upper ocean.

### 3.2.2. Upper 1000 m

Below the euphotic zone, the distribution of the dFe size classes was very different in the subtropical gyre than in the OMZ (Fig. 4 a&b). At the subtropical gyre sites, sFe maintained low concentrations down to 250 m (0.14–0.22 nmol/kg), while at the OMZ stations, in contrast, sFe had already reached elevated concentrations of 0.4–0.5 nmol/kg by 250 m. This is consistent with a deeper peak in apparent oxygen utilization (AOU) in the subtropical gyre than in the OMZ. By 700 m, maximum dFe was observed at all stations, and dFe was equally partitioned into cFe and sFe, $50 \pm 7\%$.

An intriguing pattern in dFe size partitioning was observed at 500 m depth (Fig. 5), which is the depth sampled at the core of the OMZ (also note that isopycnals were very flat near 500 m depth across the tropical North Atlantic, Fitzsimmons et al., 2013). In the end-member subtropical gyre stations (squares in Fig. 5) and OMZ stations (circles), dFe and sFe were relatively constant across all of the stations sampled: subtropical gyre stations had $\text{dFe} = 0.57 \pm 0.06$ nmol/kg and $\text{sFe} = 0.42 \pm 0.03$ nmol/kg (1SD, $n = 2$), whereas OMZ stations had $\text{dFe} = 1.16 \pm 0.06$ nmol/kg and $\text{sFe} = 0.65 \pm 0.03$ ($n = 4$). The nearly constant sFe concentrations across each of the end-member regions imply a control on sFe in each region.

Historically, the 0.02 μm filters that operationally define the sFe-cFe cutoff in this study have been used to define the Fe solubility of natural seawater (Kuma et al., 1996; Liu and Millero, 2002). In these Fe solubility experiments, excess Fe is added to a natural sample and equilibrated, after which the sample is filtered through a 0.02 μm filter to measure the maximum "truly soluble" fraction of dissolved Fe. This Fe solubility comprises both an inorganic dFe fraction dominated by $Fe(OH)_x^{3-x}{}_{(aq)}$ complexes and an organic fraction of "truly soluble" organic Fe-binding ligands. Given the near constancy of the sFe concentrations in the OMZ and subtropical gyre regions of this study, it is possible that the sFe concentrations measured may equal the Fe solubility in each end-member region: in this situation, all labile soluble ligands are saturated with Fe. Remineralization may be providing uncomplexed Fe to these low-oxygen depths that saturates any unbound soluble ligands. However, a remineralization-derived input of Fe-ligands might also be expected, and was in fact observed in the northeast Atlantic Ocean (Thuróczy et al., 2010), that would oppose the hypothesis that sFe is fully bound and equals Fe solubility, assuming at least some of these new remineralization-derived ligands are soluble. In the tropical North Atlantic, Fe solubility measurements have only been made in the euphotic zone (Schlosser and Croot, 2009), so the hypothesis that sFe equals Fe solubility in this region cannot be confirmed, and thus a cause for the near constancy of sFe is not clear.

Notably, however, only at intermediate oxygen concentrations (triangles in Fig. 5), did colloidal Fe dominate dFe at 500 m (cFe=55–60%, as opposed to <50% in the subtropical gyre and OMZ stations). The two "intermediate" samples were taken from OC449-2 station 9 and from the OMZ station (10°N, 45°W) of Bergquist et al. (2007), where dissolved oxygen concentrations were between 100–110 μmol/kg. At both stations, sFe was depressed to "gyre-like" concentrations, while dFe remained elevated to "OMZ" levels, producing the apparent cFe maximum. What is driving this unique dFe size partitioning as OMZ waters meet subtropical gyre waters? We exclude a redox explanation despite its clear link to oxygen concentrations, since at all stations of this study dissolved oxygen (minimum of ~50 μmol/kg) was high enough to favor Fe(III) over Fe(II) thermodynamically. Alternatively, remineralization and ligand-partitioning may actually be the cause for this change in dFe size partitioning: if the population of microorganisms at intermediate oxygen concentrations or in the surface waters above these regions is unique, then the size partitioning of new remineralization-produced Fe ligands may also be changing as a function of the biological population, perhaps driving the formation of enhanced organically-bound dFe into the colloidal size fraction. On the other hand, this pattern may be an abiotic function of the mixing of lower-oxygen OMZ waters with higher-oxygen subtropical gyre waters. It is clear that sFe concentrations remain depressed to subtropical gyre levels at these intermediate stations, and if sorption/aggregation rates transforming soluble Fe into colloidal Fe were higher than desorption/disaggregation to the soluble phase in this mixing zone, then cFe would be favored. This could be motivated by an increase in particle concentrations or a change in particle composition at these mixing stations around the edge of the OMZ. Regardless of the cause, colloids may be serving as a conduit of dFe loss during mixing of high dFe waters of the OMZ with the low dFe waters of the gyre. If the colloidal phase is actively aggregating, as suggested by the model of Honeyman and Santschi (1989), the partitioning of the remineralized fraction could affect the efficiency of Fe recycling, since if cFe aggregated to the particulate phase before being upwelled to the surface ocean, it would constitute a "leak" in the Fe recycling system that might not be present if the mixing zone was partitioned less into the colloidal phase.

### 3.2.3. Deep ocean

We determined the deep water size partitioning of dFe at one station in the deepest part of the eastern tropical North Atlantic basin (Station 13: 12.8°N, 33.0°W, Fig. 6a). As described in Fitzsimmons et al. (2013), Antarctic Intermediate Water (AAIW) was the main water mass near 1000 m, North Atlantic Deep Water (NADW) dominated from 1500–4000 m, and Antarctic Bottom Water (AABW) was mixed with NADW below 4000 m. In the deepest samples from 4000–5000 m, Fitzsimmons et al. (2013) observed a 0.1 nmol/kg increase in dFe compared to the shallower NADW-only depths, which they suggested might have been acquired during deep water transit through the Vema Fracture Zone, since hydrothermally-influenced water, potentially with higher Fe concentrations, has been detected near the Vema Fracture Zone (Klinkhammer et al., 1985). As can be seen in Fig. 6a, sFe concentrations at these AABW-influenced depths were not significantly different from those at the shallower, NADW-only depths, and thus the AABW increase in dFe was contributed only by the colloidal Fe phase (composing 65 ± 2% of the dFe in the deepest samples, $n = 2$). If this 0.1 nmol/kg excess dFe is hydrothermally-derived, it is unknown whether it is composed of organically-bound colloidal Fe, as would traditionally be assumed in deep ocean waters, or whether an inorganic Fe colloidal phase precipitated during venting also contributes. Regardless, this cFe would have had to escape scavenging over the > 1200 km transit from the Vema Fracture Zone to Station 13 in order for it to explain the observed increase in cFe concentrations.

In the mid-depth NADW at this site, sFe constituted 48 ± 11% of the dFe pool, and sFe concentrations were 0.34 ± 0.05 nmol/kg ($n = 2$), which compares well with the 0.35 ± 0.05 nmol/kg values reported by Bergquist et al. (2007) in the North (Fig. 6b) and South Atlantic as well as the ~0.32 nmol/kg values reported by Wu et al. (2001) near Bermuda. Even in the Atlantic sector of the Southern Ocean, at depths where NADW is detected by enhanced salinity, the same sFe values of 0.35 ± 0.02 nmol/kg were observed (Chever et al., 2010). This is in contrast to measurements in the northeast Atlantic off Portugal where sFe was only measured to be 0.16–0.21 nmol/kg in NADW (Thuróczy et al., 2010). These samples, however, were collected using a different operational definition of the sFe size fraction, a 1000 kDa membrane in a cross-flow filtration apparatus, and thus cannot be directly compared to the sFe concentrations in this

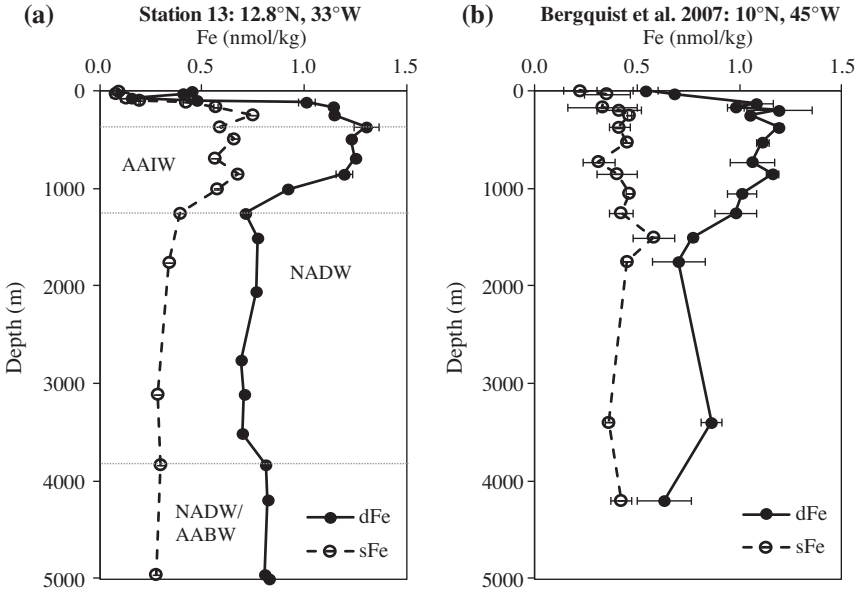


Fig. 6. (a) Full-depth profile of dissolved Fe partitioning at Station 13 in the deepest part of the eastern tropical North Atlantic basin. The depths of relevant water masses discussed in the text (with acronyms designated) are indicated with dotted lines. (b) Full-depth profile of dissolved Fe partitioning in the OMZ station from Bergquist et al. (2007) is shown for comparison. In both cases, error bars designate ±1 standard deviation on replicate sample analyses.

study, which were collected using 0.02 μm Anopore filtration (Fitzsimmons and Boyle, in review).

### 3.3. Controls on dissolved Fe size partitioning in the tropical North Atlantic

In their study on dFe size partitioning in the Atlantic Ocean, Bergquist et al. (2007) suggested that it is changes in colloidal Fe concentration that determines dFe variability in the open ocean, while soluble Fe remains invariant with depth. This pattern is clear in their data, which is reproduced in Fig. 6b: sFe is relatively constant at 0.3–0.4 nmol/kg below the euphotic zone, while dFe is at high and variable concentrations, with most of the variability contributed by changes in the colloidal phase. In contrast, however, the full-depth profile data from Station 13 of this study (Fig. 6a) shows that where dissolved Fe is enhanced in the OMZ, soluble Fe is also enhanced, and as a result both soluble and colloidal fractions contribute to the variability in the dFe profile. In fact, the sFe concentrations from all stations of OC449-2 were generally more variable than in the two stations measured by Bergquist et al. (2007; Fig. 4c–d), and at no stations in OC449-2 could sFe be considered to remain constant with depth. At the subtropical gyre site of Bergquist et al. (2007), sFe concentrations were nearly constant through the upper 1000 m, averaging $0.34 \pm 0.04$ nmol/kg (1SD, $n = 12$) over all depths sampled, while OC449-2 subtropical gyre stations reached lower sFe minima in the upper ocean (0.12–0.22 nmol/kg) and higher maxima in the deeper waters (0.4–0.5 nmol/kg; Fig. 4c). The same is true of the OMZ stations where OC449-2 stations reached a lower sFe near the chlorophyll maximum (0.1–0.15 nmol/kg) and higher sFe maxima in OMZ waters (0.6–0.7 nmol/kg) than the nearly constant $0.40 \pm 0.06$ nmol/kg ($n = 9$) measured by Bergquist et al. (2007) at their OMZ site (Fig. 4d).

Relatively invariant sFe below the euphotic zone was a major finding of the Bergquist et al. (2007) study that, combined with the dominance of cFe in the upper waters underlying dust deposition, led them to conclude that colloidal Fe dominates dFe variability throughout the ocean (Fig. 7a). The tropical North Atlantic OC449-2 stations, however, show a reliance of dFe variability on both sFe and cFe concentrations (Fig. 7b). Why do these two studies show different patterns in dFe size partitioning? One possibility is that Station 13 is farther into the OMZ than Bergquist et al.'s OMZ station and thus might receive more of a "uniquely partitioned" OMZ Fe input that is enriched in more soluble Fe than colloidal Fe. Fitzsimmons et al. (2013) used several proxies to apportion the Fe sources to the OMZ and concluded that the most likely mechanism for the enriched Fe in the broad tropical North Atlantic OMZ was enhanced remineralization of high Fe:C organic material formed in the dust-laden surface waters above, rather than advection/mixing out from an African margin Fe source. If this is true, then for a remineralization-derived "source partitioning signature" to explain the difference between dFe partitioning in the Fig. 6 profiles, there must be a difference in the microbial communities between Station 13 and Bergquist et al.'s OMZ station that would cause a change in the partitioning of remineralized Fe in the OMZ. Alternatively, the partitioning of free ligands that bind this newly remineralized material in the OMZ could be different between the two sites, favoring more soluble ligands along OC449-2 stations and more colloidal ligands at Bergquist et al.'s study site.

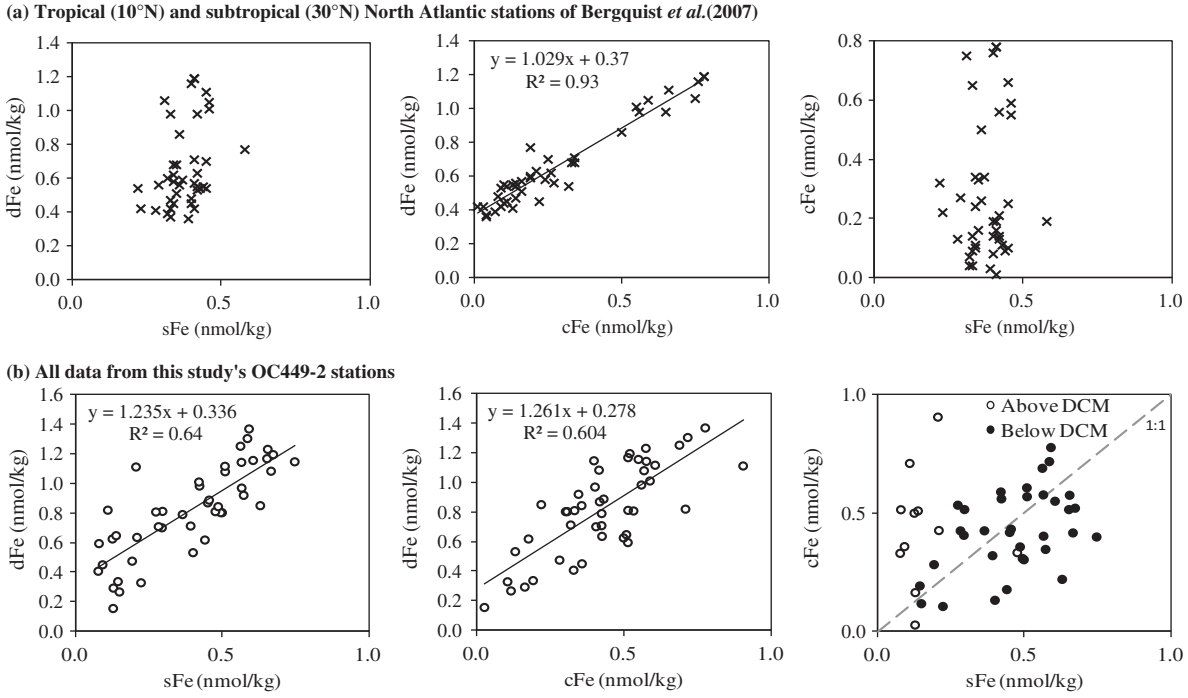


Fig. 7. dFe size partitioning in the North Atlantic stations of Bergquist et al. (2007) in (a) and this study OC449-2 (b). The relationship between sFe–dFe is shown on the left, cFe–dFe in the middle, and sFe–cFe on the right. The error in the slopes and intercepts from this study's data are ±1SE. There is no relationship between dFe and sFe in the data of Bergquist et al. (2007), while there is a statistically significant dFe–sFe relationship in the stations of this study.

However, as shown in Fig. 7b, the dFe dependence on both sFe and cFe phases in OC449-2 is not isolated only to the OMZ stations: both soluble and colloidal size fractions are variable across the entire tropical North Atlantic Ocean, including the subtropical gyre stations. The data of Bergquist et al. (2007) shows a narrower range in sFe concentrations despite a wide range in dFe concentrations, and thus only a dFe–cFe relationship can be deduced from their data (Fig. 7a). Across the wider OC449-2 span of oceanographic conditions in the tropical North Atlantic (Fig. 7b), however, sFe too was correlated with dFe variability.

We believe that the dFe partitioning pattern where both sFe and cFe contributions to dFe variability is more representative of the general tropical North Atlantic Ocean, given the wider range of sampling locations in OC449-2. We hypothesize that this more equivalent sFe-cFe partitioning is attributed to one of two mechanisms: (1) the near-equal partitioning of Fe-binding ligands in the two size fractions controls dFe size distributions directly (an "equilibrium" control of dFe size partitioning), or (2) following remineralization the exchange rates between soluble and colloidal Fe (aggregation/disaggregation or ligand exchange) set a "steady state" dFe partitioning that is nearly equivalent between the two size fractions (a kinetic control of dFe size partitioning). We suggest that the >0.8 nmol/kg dFe data of Bergquist et al. data in Fig. 7a fall off the linear dFe-sFe trend because they do not reach a steady state between aggregation/disaggregation due to their location in waters of "intermediate" oxygen concentration after mixing of OMZ and gyre waters (as discussed in Section 3.2.2).

We emphasize that a statistically significant linear slope between dFe–sFe (Fig. 7b, left panel) was observed in this OC449-2 dataset, while no previous study in the Atlantic Ocean (Bergquist et al., 2007), Northeast Atlantic (Thuróczy et al., 2010), or the Southern Ocean (Chever et al., 2010) recorded a statistically significant dFe-sFe regression. This reinforces the conclusion that soluble Fe is playing a greater role in dFe variability in the tropical North Atlantic than previously suggested. We also note that the slopes for the dFe–sFe ($1.235 \pm 0.140$, ±1SE) and dFe–cFe ($1.261 \pm 0.156$) relationships in Fig. 7 are identical, indicating that within the scatter of the regressions, soluble and colloidal Fe contribute equally (50–50%) to dissolved Fe variability. This can also be seen in the sFe–cFe plot in the right panel of Fig. 7b, where most of the points below the DCM fall on or near the 1:1 line, indicating that sFe and cFe concentrations on average contribute 50–50% of dFe variability. We note here that serial correlation (resulting from a calculation of cFe as dFe–sFe) would cause any random error in sFe to result in a random relationship between sFe and cFe, while our results show a slightly positive sFe–cFe relationship near the 1:1 sFe–cFe line for all data below the DCM. Furthermore, any systematic positive error in sFe would result in an underestimation of cFe by autocorrelation; however, we find a positive dFe–cFe correlation (Fig. 7b, middle panel) and thus discount systematic errors causing biased dFe–cFe relationships via serial correlation. The dFe–cFe slope calculated for the OC449-2 data ($1.261 \pm 0.156$) is not significantly different from the dFe-cFe slopes cited by Bergquist et al. (2007) for their Atlantic Ocean data (1.18) or Thuróczy et al., 2010 for their Northeast Atlantic data (1.16).

The near-equal slopes between dFe–sFe and dFe–cFe and the sFe–cFe relationship near the 1:1 line below the DCM both suggest that the average partitioning of marine dFe is 50–50% to the soluble and colloidal pools (when using a 0.02 μm filter), driven either by direct control of the dFe size distribution by equally partitioned Fe-binding ligands or by a steady-state exchange rate between soluble-colloidal Fe pools. However, regional Fe inputs or processes may impart additional Fe sources to one of the phases on top of this constant partitioning, while scavenging/output processes may detract from it, to produce the observed variable partitioning. An example of this is the upper ocean (DCM and above), where uniquely partitioned Fe sources (dust) and/or biological Fe processing has prevented the dFe from reaching the nearly 50–50% size partitioning observed at steady state in the rest of the water column (Fig. 7b, right panel, open circles). Additionally we believe that the data of Bergquist et al. (2007) has not reached a sFe–cFe steady state exchange because of unique processes/kinetics occurring in the OMZ-gyre mixing zone (Section 3.2.2). Whether it is abiotic rates of scavenging/aggregation or the partitioning of organic ligands that controls the observed constant dFe partitioning, and if so which Fe-ligands are most important and where do they come from, remains to be determined. The constant partitioning model is supported globally by near equal contributions of soluble and colloidal Fe to deep ocean dFe partitioning in the Atlantic, Pacific, and Southern Oceans (Wu et al., 2001; Bergquist et al., 2007; Boye et al., 2010; Chever et al., 2010).

It is clear from this and similar studies that the partitioning of dFe between soluble and colloidal phases is variable, even within the tropical North Atlantic alone, yet this partitioning has a major impact on Fe biogeochemical cycling, potentially affecting dFe bioavailability, solubility, and residence times. Unfortunately, we know very little about the chemical composition of dFe in the ocean, but it is clear from this and other size fractionation studies that soluble and colloidal Fe species cycle independently to some extent (especially in the upper ocean) and warrant further study, both in exploration of their distribution as well as in experimental constraint of their bioavailability, exchange kinetics, and scavenging potential. We rely on the assumption that the partitioning of organic Fe-binding ligands influences the observed dFe partitioning, yet of the three published studies that have measured the size fractionation of ligands using electrochemical techniques (Cullen et al., 2006; Boye et al., 2010; Thuróczy et al., 2010), none have found that ligand partitioning actually predicts the observed dFe partitioning. This either indicates that electrochemical measurements are missing a fraction of Fe-binding ligands that are active in the open ocean, or that there is a missing link between our kinetically-limited measurements of Fe-binding ligand concentration/binding strength and our thermodynamic understanding of organic ligand-binding of Fe in the open ocean. We still have much to learn about the chemical environment of dFe in the open ocean that will help us predict how Fe is solubilized and made available to marine microbes yet also is eventually scavenged to the particulate phase.

## 4. CONCLUSIONS

In this study, we investigated the partitioning of dFe between soluble and colloidal size fractions in the tropical North Atlantic and compared the distributions to the study of dFe size partitioning completed previously in the western portion of this region (Bergquist et al., 2007). We found that in the surface ocean underlying the Saharan dust plume that dFe was composed predominately of colloidal Fe, supporting the hypothesis that dust-derived Fe may be preferentially retained in the colloidal size fraction (Wu et al., 2001; Aguilar-Islas et al., 2010). At the chlorophyll maximum, colloidal Fe was minimized or disappeared completely, which is likely due to a combination of biological uptake of colloidal Fe and/or the scavenging/aggregation of cFe at this depth. At remineralization depths, colloidal Fe only dominated at intermediate oxygen concentrations of 100–110 μmol/kg, suggesting that colloidal Fe may serve as a conduit of Fe loss during mixing of OMZ and oxygenated gyre waters. In the deep ocean, dFe size partitioning averaged 50–50% between the soluble and colloidal phases. Typical NADW sFe concentrations were observed, and in deeper waters including an AABW component that appear to have acquired Fe from hydrothermal activity or some other source during passage through the Vema Fracture Zone (Fitzsimmons et al., 2013), soluble Fe did not increase coincidently, indicating that any Fe addition was contributed by the colloidal phase alone.

Most significantly, the results of this study oppose the premise that colloidal Fe alone controls the dissolved Fe variability in the open ocean. We instead propose that both soluble and colloidal Fe control dFe concentration variability and that the near-constancy of sFe with depth observed in previous studies represents either a constant open ocean dFe partitioning pattern over which regional Fe sources with unique dFe partitioning are overlain to explain the observed partitioning, or that Fe-binding ligand partitioning between the two size fractions is variable in the open ocean and directly controls dFe partitioning. This distinction warrants future exploration in studies where the size fractionation of both the Fe-binding ligands and dFe are measured together throughout the water column. In general, this study confirms that soluble and colloidal Fe have unique patterns of cycling in different ocean regions and depths, and the two size classes cycle independently to some extent, especially in the upper ocean. These global dFe partitioning distributions influence both the bioavailability and scavenging residence time of dFe in the open ocean.

## ACKNOWLEDGEMENTS

We thank Ruifeng Zhang for his help with the dissolved iron measurements as well as Richard Kayser for his efforts maintaining and deploying the MITESS units. We would also like to thank Phoebe Lam, Mark Wells, and Carl Lamborg for useful discussions about marine colloidal Fe and three anonymous reviewers for useful comments on this manuscript. Excellent marine support was offered by the officers and crew of the *R/V Oceanus*. Finally, we thank Reiner Schlitzer and his group for sharing the Ocean Data

View graphics program. J.N. Fitzsimmons was funded by a National Science Foundation Graduate Research Fellowship (NSF Award #0645960), and this work was funded by NSF OCE-07020278 and the Center for Microbial Oceanography: Research and Education (NSF-OIA Award #EF-0424599).

## APPENDIX A. SUPPLEMENTARY DATA

Supplementary data associated with this article can be found, in the online version, at http://dx.doi.org/10.1016/j.gca.2013.10.032.

## REFERENCES

Aguilar-Islas A. M., Wu J., Rember R., Johansen A. M. and Shank L. M. (2010) Dissolution of aerosol-derived iron in seawater: leach solution chemistry, aerosol type, and colloidal iron fraction. *Mar. Chem.* **120**, 25–33.

Barbeau K. and Moffett J. W. (2000) Laboratory and field studies of colloidal iron oxide dissolution as mediated by phagotrophy and photolysis. *Limnol. Oceanogr.* **45**, 827–835.

Barbeau K., Moffett J. W., Caron D. A., Croot P. L. and Erdner D. L. (1996) Role of protozoan grazing in relieving iron limitation of phytoplankton. *Nat. Geosci.* **380**, 61–64.

Bell J., Betts J. and Boyle E. (2002) MITESS: a moored in situ trace element serial sampler for deep-sea moorings. *Deep-Sea Res. Part I-Oceanogr Res Pap.* **49**, 2103–2118.

Bergquist B. A. and Boyle E. A. (2006) Dissolved iron in the tropical and subtropical Atlantic Ocean. *Global Biogeochem. Cycles* **20**, 14.

Bergquist B. A., Wu J. and Boyle E. A. (2007) Variability in oceanic dissolved iron is dominated by the colloidal fraction. *Geochim. Cosmochim. Acta* **71**, 2960–2974.

Boye M., Nishioka J., Croot P., Laan P., Timmermans K. R., Strass V. H., Takeda S. and de Baar H. J. W. (2010) Significant portion of dissolved organic Fe complexes in fact is Fe colloids. *Mar. Chem.* **122**, 20–27.

Bruland K. W. and Lohan M. C. (2003) Controls of trace metals in seawater. In *Treatise On Geochemistry* (eds. K. K. Turekian and H. D. Holland). Elsevier Science Ltd., Cambridge, United Kingdom.

Chen M. and Wang W. X. (2001) Bioavailability of natural colloid-bound iron to marine plankton: influences of colloidal size and aging. *Limnol. Oceanogr.* **46**, 1956–1967.

Chever F., Bucciarelli E., Sarthou G., Speich S., Arhan M., Penven P. and Tagliabue A. (2010) Physical speciation of iron in the Atlantic sector of the Southern Ocean along a transect from the subtropical domain to the Weddell Sea Gyre. *J. Geophys. Res.* **115**, C10059.

Cullen J. T., Bergquist B. A. and Moffett J. W. (2006) Thermodynamic characterization of the partitioning of iron between soluble and colloidal species in the Atlantic Ocean. *Mar. Chem.* **98**, 295–303.

Fitzsimmons J. N. and Boyle E. A. (2012) An intercalibration between the GEOTRACES GO-FLO and the MITESS/Vanes sampling systems for dissolved iron concentration analyses (and a closer look at adsorption effects). *Limnol. Oceanogr.: Methods* **10**, 437–450.

Fitzsimmons, J. N. and Boyle, E. A. (in review) Assessment and comparison of Anopore and cross flow filtration methods for the determination of dissolved iron size fractionation into soluble and colloidal phases in seawater. *Limnol. Oceanogr.: Methods*.

Fitzsimmons J. N., Zhang R. and Boyle E. A. (2013) Dissolved iron in the tropical North Atlantic oxygen minimum zone. *Mar. Chem.* **154**, 87–99.

Gledhill, M. and Buck, K. N. (2012) The organic complexation of iron in the marine environment: a review. *Front. Microbiol.: Microbiol. Chem.* **3**, Article 69.

Honeyman B. D. and Santschi P. H. (1989) A Brownian-pumping model for oceanic trace metal scavenging: evidence from Th isotopes. *J. Mar. Res.* **47**, 951–992.

Hunter K. A. and Boyd P. W. (2007) Iron-binding ligands and their role in the ocean biogeochemistry of iron. *Environ. Chem.* **4**, 221–232.

Klinkhammer G., Rona P., Greaves M. and Elderfield H. (1985) Hydrothermal manganese plumes in the Mid-Atlantic Ridge rift valley. *Nature* **314**, 727–731.

Kuma K., Nishioka J. and Matsunaga K. (1996) Controls on iron(III) hydroxide solubility in seawater: the influence of pH and natural organic chelators. *Limnol. Oceanogr.* **41**, 396–407.

Lee J.-M., Boyle E. A., Echegoyen-Sanz Y., Fitzsimmons J. N., Zhang R. and Kayser R. A. (2011) Analysis of trace metals (Cu, Cd, Pb, and Fe) in seawater using single batch Nitrilotriacetate resin extraction and isotope dilution inductively coupled plasma mass spectrometry. *Anal. Chim. Acta* **686**, 93–101.

Liu X. and Millero F. J. (2002) The solubility of iron in seawater. *Mar. Chem.* **77**, 43–54.

Mahowald, N., Baker, A. R., Bergametti, G., Brooks, N., Duce, R. A., Jickells, T., Kubilay, N., Prospero, J. M., and Tegen, I. (2005) Atmospheric global dust cycle and iron inputs to the ocean. *Global Biogeochem. Cycles* **19**, GB4025.

Martin J. H. and Fitzwater S. E. (1988) Iron deficiency limits phytoplankton growth in the north-east Pacific subarctic. *Nature* **331**, 341–343.

Martinez J. S., Haygood M. G. and Butler A. (2001) Identification of a natural desferrioxamine siderophore produced by a marine bacterium. *Limnol. Oceanogr.* **46**, 420–424.

Martinez J. S., Carter-Franklin J. N., Mann E. L., Martin J. D., Haygood M. G. and Butler A. (2003) Structure and membrane affinity of a suite of amphiphilic siderophores produced by a marine bacterium. *Proc. Nat. Acad. Sci.* **2003**, 3754–3759.

Millero F. J. (1998) Solubility of Fe(III) in seawater. *Earth Planet. Sci. Lett.* **154**, 323–329.

Moffett, J. W. (2001) Transformations among different forms of iron in the ocean. In *The Biogeochemistry of Iron in Seawater* (eds. D. R.Turner and K. A. Hunter). John Wiley & Sons, West Sussex, England.

Morel F. M. M., Milligan A. J. and Saito M. A. (2003) Marine bioinorganic chemistry: the role of trace metals in the oceanic cycles of major nutrients. In *Treatise on Geochemistry* (eds. K. K. Turekian and H. D. Holland). Elsevier Science Ltd., Cambridge, United Kingdom.

Nishioka, J., Takeda, S., Kudo, I., Tsumune, D., Yoshimura, T., Kuma, K., and Tsuda, A. (2003) Size-fractionated iron distributions and iron-limitation processes in the subarctic NW Pacific. *Geophys. Res. Lett.* **30**.

Rich H. W. and Morel F. M. M. (1990) Availability of well-defined iron colloids to the marine diatom *Thalassiosira weissflogii*. *Limnol. Oceanogr.* **35**, 652–662.

Roy E. G., Wells M. L. and King D. W. (2008) Persistence of iron(II) in surface waters of the western subarctic Pacific. *Limnol. Oceanogr.* **53**, 89–98.

Rue E. L. and Bruland K. W. (1995) Complexation of iron(III) by natural organic ligands in the Central North Pacific as determined by a new competitive ligand equilibration/adsorptive cathodic stripping voltammetric method. *Mar. Chem.* **50**, 117–138.

Schlosser C. and Croot P. L. (2009) Controls on seawater Fe(III) solubility in the Mauritanian upwelling zone. *Geophys. Res. Lett.* **36**, L18606.

Thuróczy C. E., Gerringa L. J. A., Klunder M. B., Middag R., Laan P., Timmermans K. R. and de Baar H. J. W. (2010) Speciation of Fe in the Eastern North Atlantic Ocean. *Deep Sea Res. Part I* **57**, 1444–1453.

Ussher S. J., Achterberg E. P., Sarthou G., Laan P., de Baar H. J. W. and Worsfold P. J. (2010) Distribution of size fractionated dissolved iron in the Canary Basin. *Mar. Environ. Res.* **70**, 46–55.

Wells M. L. and Goldberg E. D. (1991) Occurrence of small colloids in sea water. *Nature* **353**, 342–344.

Wells M. L. and Goldberg E. D. (1992) Marine submicron particles. *Mar. Chem.* **40**, 5–18.

Wilhelm S. W. and Trick C. G. (1994) Iron-limited growth of cyanobacteria – multiple siderophore production is a common response. *Limnol. Oceanogr.* **39**, 1979–1984.

Wu J., Boyle E. A., Sunda W. G. and Wen L. (2001) Soluble and colloidal iron in the oligotrophic North Atlantic and North Pacific. *Science* **293**, 847–849.

*Associate editor:* Derek Vance